

equivalent electrical length of 90° at two frequencies because of its nonuniform impedance. Figure 1(b) shows the proposed configuration of the dual-wideband bandpass filter with order $N = 2$. Figure 1(c) illustrates a circuit equivalent to that in Fig. 1(b) while the series-connected parallel LC resonator structure is constructed to perform the two resonance frequencies. When the resonators $L_f C_f$ resonate at ω_f (the first center frequency) and $L_s C_s$ resonate at ω_s (the second center frequency), their input impedances approach infinity. Thus, composite LC resonators function like open circuits at ω_f and ω_s , thereby allowing the signal to pass through and achieve the dual-passband response.

With reference to Fig. 2, the input admittances of the shorted SIR and its equivalent circuit are given by

$$Y_{SIR} = j \frac{Z_2 \tan \theta_1 \tan \theta_2 - Z_1}{Z_1 (Z_1 \tan \theta_1 + Z_2 \tan \theta_2)} \quad (1a)$$

$$Y_c = \frac{j C_f C_s (\omega^2 - \omega_f^2)(\omega^2 - \omega_s^2)}{\omega [C_s (\omega^2 - \omega_s^2) + C_f (\omega^2 - \omega_f^2)]} \quad (1b)$$

where $C_f = g_f / \omega_f \Delta_f$, $C_s = g_s / \omega_s \Delta_s$, $\Delta_{f,s}$ are the fractional bandwidths of the first and second passband, respectively, and g_i is the low-pass prototype element value. Notably, the resonant frequencies of ω_f and ω_s can be determined by using the resonant condition $Y_{SIR} = 0$. Further, the susceptance slope parameter [11] can be used to ensure that the proposed SIR and its equivalent circuit have the same bandwidth. Based on the susceptance slope and the resonant condition at ω_f and ω_s , four simultaneous equations are formed

$$\frac{Z_2 \tan \theta_1 \tan \theta_2 - Z_1}{Z_1 (Z_1 \tan \theta_1 + Z_2 \tan \theta_2)} = 0 \quad (2a)$$

$$\frac{Z_2 \tan(r_f \theta_1) \tan(r_f \theta_2) - Z_1}{Z_1 [Z_1 \tan(r_f \theta_1) + Z_2 \tan(r_f \theta_2)]} = 0 \quad (2b)$$

$$\frac{Z_1^2 \theta_1 \cos^2 \theta_2 + Z_2^2 \theta_1 \sin^2 \theta_2 + Z_1 Z_2 \theta_2}{2 Z_1 (Z_1 \sin \theta_1 \cos \theta_2 + Z_2 \cos \theta_1 \sin \theta_2)^2} = \frac{g_f}{\Delta_f} \quad (2c)$$

$$\frac{r_f [Z_1^2 \theta_1 \cos^2(r_f \theta_2) + Z_2^2 \theta_1 \sin^2(r_f \theta_2) + Z_1 Z_2 \theta_2]}{2 Z_1 [Z_1 \sin(r_f \theta_1) \cos(r_f \theta_2) + Z_2 \cos(r_f \theta_1) \sin(r_f \theta_2)]^2} = \frac{g_s}{\Delta_s} \quad (2d)$$

where $r_f = \omega_f / \omega_s$ denotes the frequency ratio. Notably, θ_1 and θ_2 in (2) are defined at ω_f . The center frequencies and bandwidths of the proposed filter are controllable via impedance changes and SIR length as shown in (2). By eliminating Z_1 and Z_2 , the four equations (2a)-(2d) are further simplified to two equations

$$r_f r_b [\theta_2 \cos^2(r_f \theta_1) \csc^2(r_f \theta_2) + \theta_1 \cot(r_f \theta_1) \cot(r_f \theta_2)] = \theta_2 \cos^2 \theta_1 \csc^2 \theta_2 + \theta_1 \cot \theta_1 \cot \theta_2 \quad (3a)$$

$$\tan \theta_1 \tan \theta_2 = \tan(r_f \theta_1) \tan(r_f \theta_2) \quad (3b)$$

where r_b is the bandwidth ratio Δ_s to Δ_f . Solving for θ_1 and θ_2 simultaneously by using a simple root-searching program and substituting into (2), one can obtain the values of Z_1 and Z_2 .

The calculated results in Fig. 3(a) show the electrical lengths θ_1 and θ_2 versus the frequency ratio r_f . The range of r_f is chosen from 1.1 to 2.9, which covers most of the design objectives. In Fig. 3(a), there are three cases in which product $r_f \cdot r_b = 0.8, 1, \text{ and } 1.2$. It is found that $\theta_1 > \theta_2$ for $r_f \cdot r_b < 1$ and $\theta_1 = \theta_2$ for $r_f \cdot r_b$

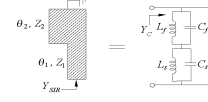
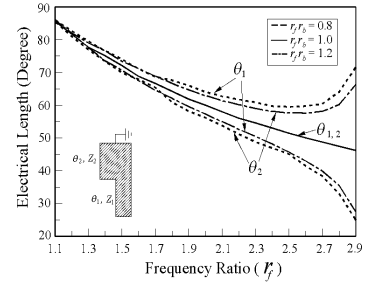
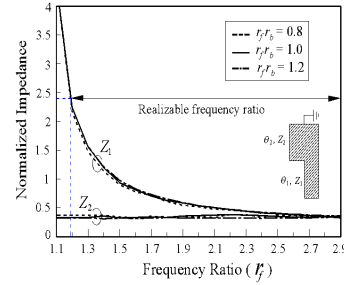


Fig. 2 Equivalence of shorted SIR and series-connected parallel LC resonators.



(a)



(b)

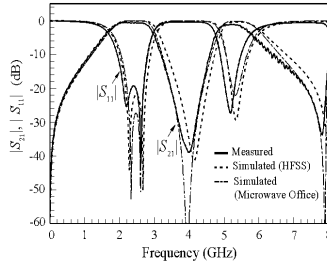
Fig. 3 (a) Electrical lengths θ_1 and θ_2 of shorted SIR versus r_f . (b) Normalized impedances Z_1 and Z_2 versus r_f .

$= 1$. When $r_f \cdot r_b > 1$, the design curves of θ_1 and θ_2 become reversed ($\theta_1 < \theta_2$) to the solid curve $r_f \cdot r_b = 1$. Figure 3(b) plots the normalized impedances Z_1 and Z_2 versus r_f with the element value of $g_1 = 1.4142$ (second-order maximally flat low-pass prototype) and $\Delta_f = 60\%$. The value of Z_1 increases exponentially as r_f decreases while Z_2 remains almost constant. Neither Z_1 or Z_2 are sensitive to the product $r_f \cdot r_b$. Since Z_1 always exceeds Z_2 , the upper section of the proposed SIR should have a wider line width than the lower section to

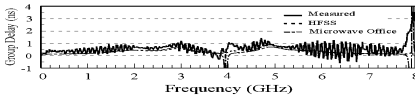
achieve dual-passband performance. When r_f approaches three, Fig. 3 reveals the tendency of $Z_1 \approx Z_2 \approx 0.33$ and $\theta_1 + \theta_2 \approx 90^\circ$ in which the proposed SIR becomes the conventional $\Lambda_g/4$ uniform stub.

Due to the highest practical limit of impedance realization (120Ω typically), as shown in Fig. 3(b), the frequency ratio is realizable for nearly the entire range except $r_f < 1.19$. This wide achievable range is very helpful to construct dual-band filters with arbitrary frequency ratio. Notably, it is also found that the solutions of Z_1 and Z_2 don't exist or become impractical if $\Delta_{f,s}$ are less than 30%. The reason is that the ratio of Z_1/Z_2 is reduced to one as the bandwidth reduces, which conflicts with dual band requirement (requires nonuniform impedance). Thus, the proposed structure is particularly appropriate for wide passband applications.

The admittance inverter between SIRs can be calculated by using $J_{i,i+1} = g_0 g_1 / \sqrt{g_i g_{i+1}}$, and the simplified dual-band structure presented in [12] is adopted to realize the J inverter for the proposed filter.



(a)



(b)

Fig. 4 (a) $|S_{21}|$ and $|S_{11}|$ responses of the proposed dual-wideband bandpass filter. (b) Group delay. $Z_1 = 23.35 \Omega$, $\theta_1 = 55.63^\circ$, $Z_2 = 16 \Omega$, $\theta_2 = 57.87^\circ$, $Z_3 = 59.73 \Omega$, and $\theta_3 = 56.84^\circ$.

III. SIMULATION AND MEASUREMENT RESULTS

Validity of the proposed structure was tested experimentally by constructing a second-order maximally flat dual-wideband bandpass filter on 25N substrates with $\epsilon_r = 3.38$, $\tan \delta = 0.0025$, and a thickness of 0.762 mm. The central frequencies of the dual passbands were designed at 2.4 GHz and 5.2 GHz with $\Delta_f = 60\%$ and $\Delta_s = 30\%$, respectively, to match the WLAN specifications. Solving (2) and (3) with $g_1 = 1.4142$, $r_f = 2.17$, and $r_b = 0.5$ revealed that the design parameters for SIR are $Z_1 = 23.35 \Omega$, $\theta_1 = 55.63^\circ$, $Z_2 = 16 \Omega$, and $\theta_2 = 57.87^\circ$.

The design parameters of the J inverter are $Z_3 = 59.73 \Omega$ and $\theta_3 = 56.84^\circ$. The calculated circuit dimensions and simulated responses of the experimental filter were then obtained by using the full-wave EM simulator HFSS. Simulated results from the circuit simulator Microwave Office using the chosen ideal transmission line parameters were also plotted for comparison.

Figure 4(a) shows the simulated and measured S -parameters. The dual-band bandpass response was obtained, and there is good agreement between simulated and measured responses. Measured central frequencies were 2.3 and 5.25 GHz with bandwidths of 54% and 20%, respectively. The bandwidths were decreased mainly because the open stubs of the dual-band inverter were ignored. Notably, the bandwidths are wider than those of dual-band bandpass filters presented in [2], [4], [5], [8], [10]. In-band return loss and insertion loss of this filter were better than 20 dB and 0.8 dB, respectively. As Fig. 4(b) shows, the measured group delay in the passband was small and ranged from 0.5 to 1 ns. Figure 1(b) depicts a photograph of the fabricated filter, and the circuit area was about $24 \times 24 \text{ mm}^2$. In our further studies, the dual bandwidths of the proposed filter can up to 60% and 67% centered at 3.7 GHz and 9 GHz, respectively, which is not shown here for conciseness.

IV. CONCLUSIONS

This work presents a novel dual-wideband bandpass filter using short-circuited stepped-impedance resonators. The circuit possesses two wide passbands with controllable center frequencies and bandwidths. Both dual-band performance and compact size are achieved by using dual-band SIRs instead of conventional single-band quarter-wavelength shorted stubs. The synthesis method was developed and its effectiveness was demonstrated by synthesizing an experimental filter.

REFERENCES

- [1] X. Guan, Z. Ma, P. Cai, Y. Kobayashi, T. Anada, and G. Hagiwara, "Synthesizing microstrip dual-band bandpass filters using frequency transformation and circuit conversion technique," *IEICE Trans. Electron.*, vol. E89-C, no.4, pp. 495-502, April 2006.
- [2] C.-C. Chen, "Dual-band bandpass filter using coupled resonator pairs," *IEEE Microw. Wireless Compon. Lett.*, vol. 15, pp. 259-261, April 2005.
- [3] J.-X. Chen, T. Y. Yum, J.-L. Li, and Q. Xue, "Dual-mode dual-band bandpass filter using stacked-loop structure," *IEEE Microw. Wireless Compon. Lett.*, vol. 16, pp. 502-504, Sept. 2006.
- [4] C.-M. Tsai, H.-M. Lee, and C.-C. Tsai, "Planar filter design with fully controllable second passband," *IEEE Trans. Microwave Theory Tech.*, vol. 53, pp. 3429-3439, Nov. 2005.
- [5] H.-Y. Anita Yim and K.-K. Michael Cheng, "Novel dual-band planar resonator and admittance inverter for filter design and applications," in *IEEE MTT-S Int. Microwave Symp. Dig.*, pp. 2187-2190, 2005.
- [6] Z. Ma, T. Shimizu, Y. Kobayashi, T. Anada, and G. Hagiwara, "Novel compact dual-band bandpass filters using composite resonators to obtain separately controllable passbands," 2006 *Asia-Pacific Microwave Conference Proceedings*, pp. 1814-1817, Dec. 2006.
- [7] J.-T. Kuo, T.-H. Yeh, and C.-C. Yeh, "Design of microstrip bandpass filters with a dual-passband response," *IEEE Trans. Microwave Theory Tech.*, vol. 53, pp. 1331-1337, April 2005.
- [8] M.-H. Weng, H.-W. Wu, and Y.-K. Su, "Compact and low loss dual-band bandpass filter using pseudo-interdigital stepped impedance resonators

- for WLANs," *IEEE Microw. Wireless Compon. Lett.*, vol. 17, pp. 187-189, March 2007.
- [9] S.-F. Chang, Y.-H. Jeng, and J.-L. Chen, "Dual-band step-impedance bandpass filter for multimode wireless LANs," *Electron. Lett.*, vol. 40, pp. 38-39, Jan. 2004.
- [10] Y. P. Zhang and M. Sun, "Dual-band microstrip bandpass filter using stepped-impedance resonators with new coupling schemes," *IEEE Trans. Microwave Theory Tech.*, vol. 54, pp. 3779-3785, Oct. 2006.
- [11] G. L. Matthaei, L. Young and E. M. T. Johns, *Microwave Filters, Impedance Matching Networks, and Coupling Structures*. Norwood MA: Artech House, 1980.
- [12] K.-S. Chin, J.-H. Yeh, and S.-H. Chao, "Compact dual-band bandstop filters using stepped-impedance resonators," *IEEE Microwave and Wireless Components Letters*, vol. 17, no. 12, pp. 849-851, Dec. 2007.